Binding Studies of Molecular Linkers to ZnO and MgZnO Nanotip Films

Olena Taratula,[†] Elena Galoppini,*[,†] Dong Wang,[†] Dorothy Chu,[†] Zheng Zhang,[‡] Hanhong Chen,[‡] Gaurav Saraf,[‡] and Yicheng Lu[‡]

Chemistry Department, Rutgers University, 73 Warren Street, Newark, New Jersey 07102, and Electrical and Computer Engineering Department, Rutgers University, 94 Brett Road, Piscataway, New Jersey 08854

Received: December 2, 2005; In Final Form: January 27, 2006

Two bifunctional linkers, a rigid-rod *p*-ethynyl-isophthalic acid capped with a Ru(II)−polypyridyl complex and 3-mercaptopropionic acid, were covalently bound to ZnO nanotip films grown by metal−organic chemical vapor deposition (MOCVD) technology. This highly vertically aligned, crystalline form of ZnO had not been functionalized before. The binding was studied by Fourier transform (FT) IR and UV spectroscopies and probed, in the case of the Ru complex, by static and dynamic fluorescence quenching. The molecules did bind through the carboxylic acid groups, and the FT-IR attenuated total reflectance spectra are indicative of a bidentate carboxylate binding mode. Other molecules (heptanoic acid, isophthalic acid, and trimethoxy(2-phenylethyl)silane) were also bound to the ZnO nanotips. A comparison was made with epitaxial ZnO films grown by MOCVD and ZnO mesoporous films prepared from colloidal solutions to investigate the effect of the ZnO morphology. The ZnO nanotips were excellent binding substrates, particularly for the rigid-rod linker. Since ZnO films are etched at low pH (<4), novel nanotip films made of ternary $Mg_xZn_{1-x}O$, which is formed by alloying ZnO with MgO and is more resistant to acids, were developed. The $Mg_xZn_{1-x}O$ nanotip films were employed to use linkers with acidic groups and to study the effect of pH pretreatment of the surface on the binding.

Introduction

Zinc oxide (ZnO) is a wide band gap semiconductor ($E_g \approx 3.32$ eV at room temperature) that has been increasingly studied as a material for numerous applications, including light-emitting diodes,[1] UV detectors,[2] sensors,[3] and photovoltaics.[4] Through proper doping, ZnO can be made transparent and conductive, piezoelectric, or ferromagnetic. ZnO crystallizes in the wurtzite structure. ZnO nanostructures with diameters of several nanometers, which are on the same order as the exciton Bohr radii, display quantum-confinement effects.[5] Key physical properties of ZnO, such as conductivity, energy band gap, and chemical and optical properties can be modified by doping or alloying with other metal oxides.[6] Table 1 lists key properties of ZnO.[5b] In addition to ZnO colloidal solutions and mesoporous films[7] prepared from nanoparticles, numerous other ZnO nanostructures, for instance, "nanowires",[8] "nanorods",[9] "nanopillars",[10] and "nanobelts"[11] have been synthesized by thermal evaporation and condensation, hydrolysis of Zn(II) salts (sol−gel methods), electrodeposition, and other methods. Lu and co-workers have developed metal−organic chemical vapor deposition (MOCVD) techniques to grow single-crystalline ZnO "nanotips" on various substrates, including sapphire, GaN, Si, quartz, Au, glass, etc.[12] These vertically aligned nanotips are grown at ∼400 °C,[12] and their properties can be tailored through proper doping.

After the pioneering study in the early 1970s,[13] the past decade has seen a surge of interest in the binding of dyes and redox-active molecules to mesoporous films of metal oxide nanoparticles (TiO_2, SnO_2, ZnO, etc.) prepared by sol−gel methods for photovoltaics and other applications.[14] While the functionalization of ZnO nanoparticles prepared by the hydrolysis of Zn(II) salts, and therefore in the presence of water and electrolytes that can physisorb to the surface, requires conditions similar to those reported for other metal oxide colloids, the functionalization of the of ZnO nanotips grown by MOCVD remains largely unexplored.[3d,e,15]

TABLE 1: Selected Properties of ZnO[5b]

properties	parameters
crystal structure	wurtzite
space group	$P_6 3mc$
lattice constants at 300K (nm)	$a = 0.32495$ $c = 0.52069$ $c/a = 1.602$ $u = 0.3825$
thermal expansion coefficient (10^{-6}/K)	$a = 6.5$; $c = 3.02$
density at 300 K (g/cm^3)	5.606
energy band gap (direct band gap at 300 K, eV)	3.37
band gap temperature coefficient (eV/K)	2.9×10^{-4}
exciton binding energy (meV)	60
electron mobility (cm^2 V^{-1} S^{-1}) at 300 K	205
hole mobility (cm^2 V^{-1} S^{-1}) at 300 K	180
saturation electron drift velocity (10^7 cm/S)	3
static dielectric constant	8.47
index of refraction	2.09 (0.45 μm)

In this paper, we report for the first time the functionalization of Lu's single-crystalline ZnO nanotips (termed in this paper ZnO−N) in a systematic binding study of small molecules with functional groups that are known to form covalent bonds with metal oxides nanoparticles:[16] COOH, SH, $SiOMe_3$, $SiCl_3$, and $PO(OH)_2$. The structures of the compounds are shown in Figure 1. Rigid-rod Ru(II)−polypyridyl complexes **1**[17a,c] and **2**[20] were synthesized in our laboratory, and **3**−**11** are commercially available compounds. The main objective of this work was to

* Author to whom correspondence should be addressed. Phone: (973) 353-5317. Fax: (973) 258-0326. E-mail: galoppin@andromeda.rutgers.edu.
[†] Chemistry Department.
[‡] Electrical and Computer Engineering Department.

10.1021/jp0570317 CCC: $33.50
Published on Web 03/11/2006

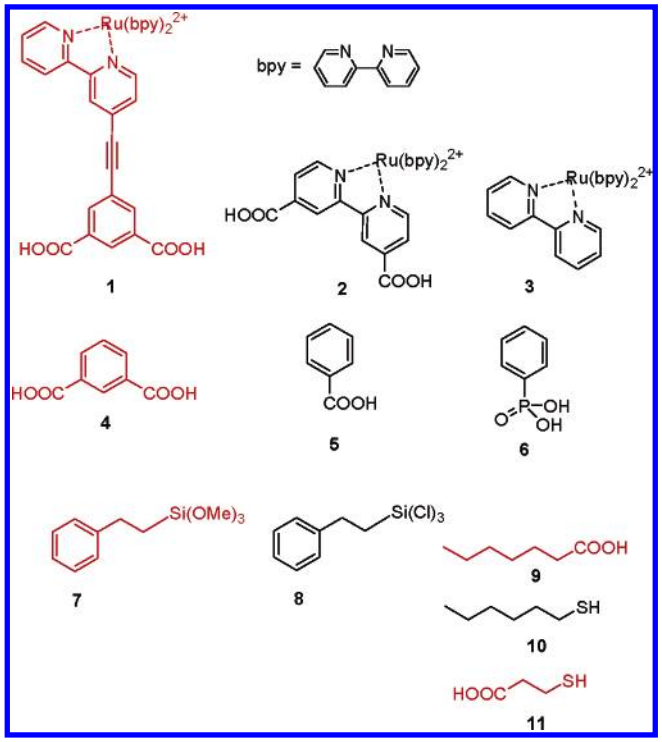

Figure 1. Compounds employed in the binding study. The compounds that did bind to the ZnO nanotips are shown in red.

CHART 1

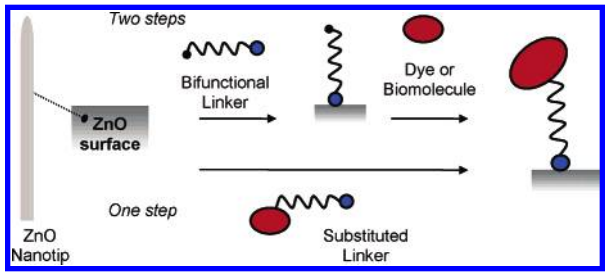

use simple molecules as models to determine which functional groups would bind to ZnO nanotips. In particular, we were interested in employing *bifunctional linkers*, preferably rigid, having one group that attaches to the surface while leaving a second one available for further functionalization of the nanotips. Alternatively, the surface functionalization could be done in one step by using a functionalized linker, as represented in Chart 1. The ability to functionalize the nanotips would lead to numerous applications, for instance, photovoltaics with a highly ordered and high surface area photoanode or new ZnO-based integrated, multimode and multifunctional sensor technology to achieve higher accuracy and sensitivity than existing sensors. This sensor technology would have broad biological and environmental applications.[3]

The binding of **1**−**11** to the nanotips was probed using one or more of the spectroscopic techniques that are typically used to study the functionalization of TiO_2 semiconductor nanoparticles. Specifically, we employed Fourier transform infrared attenuated total reflectance (FT-IR-ATR) to probe the binding of nonchromophoric molecules and UV−vis and fluorescence quenching studies, in addition to FT-IR, for Ru−polypyridyl dyes **1**−**3**. These dyes, upon photoexcitation, are expected to exhibit fluorescence quenching when bound to ZnO. For comparison, the binding of **1**−**11** was also performed on colloidal ZnO films (termed in this paper ZnO−C) and epitaxial ZnO films (termed ZnO−F).

Experimental Procedures

ZnO Nanotips and ZnO Epitaxial Films by MOCVD.[12] The growth of ZnO nanotips was carried out in a vertical flow, rotating disk MOCVD reactor. Diethylzinc (DEZn) and oxygen were used as the Zn metal−organic source and oxidizer, respectively. The detailed description of the MOCVD system was reported elsewhere.[18] Various substrates were used for ZnO nanotip growth, including glass, Si, c-sapphire, and GaN. R−Al_2O_3 ($01\bar{1}2$) was used as the substrate for the growth of a-plane ($11\bar{2}0$) ZnO epitaxial films (ZnO−F). The growth temperature was in the range of 400−500 °C, and the typical growth rate was kept at ∼1.0 μm per hour. Field emission scanning electron microscopy (FESEM) images of the ZnO nanotips (ZnO−N) are shown in Figures 2b and 2c and of ZnO−F films in Figure 2a.

The ZnO nanotips are single-crystalline, usually measuring ∼5 nm at the top, ∼70 nm at the bottom, and ∼500 nm in length. They are aligned perpendicularly to the substrate surface. Variations in the MOCVD growth conditions can provide morphology control of the ZnO nanotips. It is possible, for instance, to vary the spacing between individual nanotips (from 40 to 100 nm), their length (from less than 100 to over 6000 nm), and the top end feature (from sharp end ø < 5 nm to rounded tips). The ZnO−N is transparent from 370 nm into infrared spectral regions (Figure 3). Electrical properties, absorption spectrum, resistance to acids, and other properties (Table 1) can be tuned by doping or alloying.[6] For instance, doping ZnO with Al or Ga forms highly transparent and conductive oxides (TCOs), while alloying ZnO with MgO in the 5−10% range forms ternary compounds $Mg_xZn_{1-x}O$, which provide increased resistance to acids and band gap tuning toward the UV from ∼3.3 to ∼4.0 eV.

Preparation of ZnO Films from Colloidal Nanoparticles. This preparation was based on published methodologies.[7a,19] $Zn(CH_3COO)_2{\cdot}2H_2O$ (1.10 g) was dissolved in absolute ethanol (50 mL) and refluxed at 80 °C for 2 h under nitrogen, then cooled to room temperature. The condenser was replaced with a drying tube during cooling. To this solution tetramethylammonium hydroxide (TMAOH) (2.1 mL) was added, and upon addition of TMAOH, the solution became cloudy. Sonication (∼15 min) produced a transparent solution. This was concentrated to about 1 mL to give a viscous liquid that was cast as a film on the glass slides using the doctor blade technique. The film was calcinated in a furnace for 30 min at 350 °C (the organic components are burned in this process) and then cooled to room temperature. Uniform and optically transparent films were obtained with this method.

Binding. Typical binding procedures for the ZnO−F and ZnO−N involved placing the films in a solution of **1**−**11** in a suitable solvent (CH_3CN, THF, EtOH, or water, depending on the solubility of the compounds) overnight. Various concentrations, between 2 and 25 mM, were used for most compounds. Typical concentrations were 2 mM. The pH of the solutions was measured in each case. The films were thoroughly rinsed and then immersed in pure solvent for 1 h. This was repeated several times until desorption of weakly bound or physisorbed molecules was no longer detected. Typical binding procedures for the ZnO−C films were similar. Before binding, each ZnO−C film was placed in an oven for 30 min at 110 °C to remove moisture. The films were immersed in a ∼2−5 mM acetonitrile solution of the dye overnight, then repeatedly rinsed with acetonitrile. All types of films, prior to and after binding, were stored in small containers placed in a desiccator and in the dark.

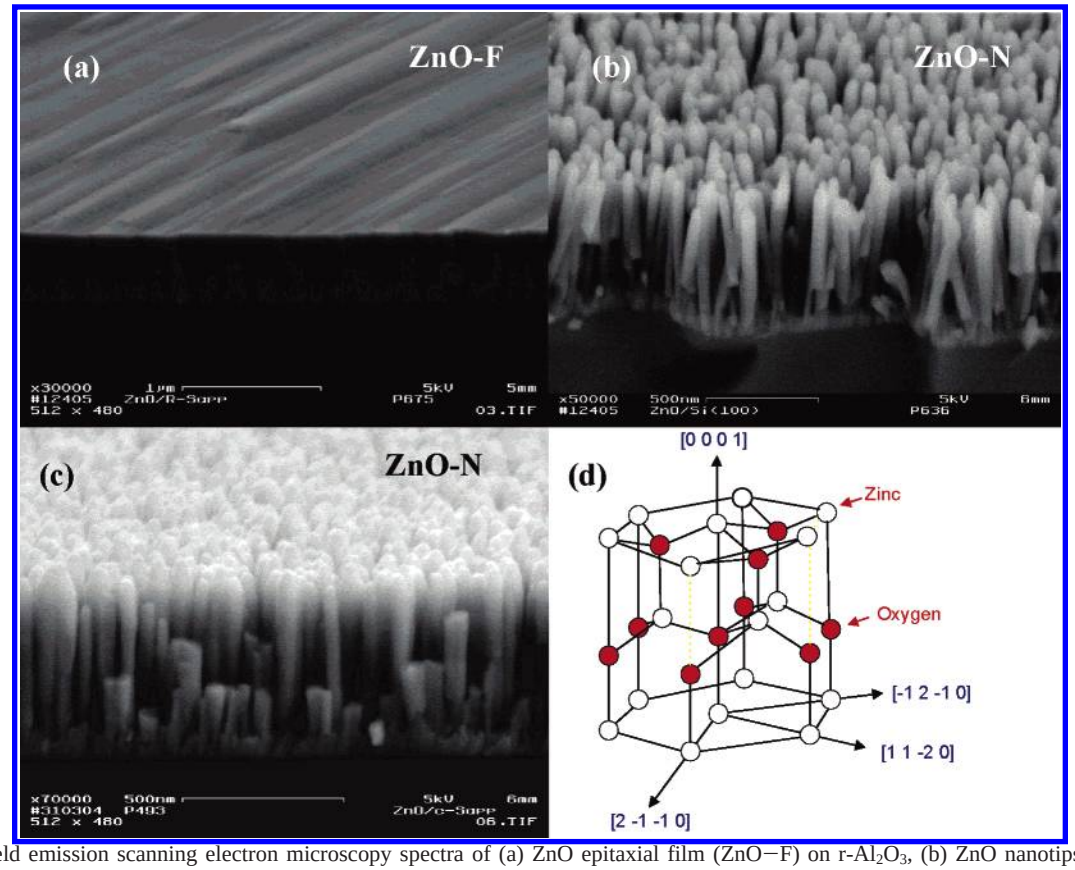

Figure 2. Field emission scanning electron microscopy spectra of (a) ZnO epitaxial film (ZnO−F) on r-Al_2O_3, (b) ZnO nanotips (ZnO−N) on Si(100), (c) ZnO nanotips on c-Al_2O_3, and (d) ZnO Wurtzite crystal structure.

No changes in the IR, UV, and fluorescence spectra were observed in bound films that were over 1 year old.

Materials. Ru complexes **1**[17a,c] and **2**[20] were synthesized as described in the literature. Compounds **3**−**11** were purchased from commercial sources and used as received. Acetonitrile was spectroscopic grade, and absolute ethanol (200 proof) and deionized ultrafiltered water were employed. Tetrahydrofuran (THF) was purchased anhydrous from Fisher, then distilled from sodium/benzophenone immediately prior to use.

Spectroscopy. Ground state UV−vis absorbance measurements were performed on a Varian Cary-500. Fluorescence emission spectra were collected on a Varian Cary-Eclipse. Single attenuated reflectance infrared (FT-IR-ATR) spectra were performed on a Thermo Electron Corporation Nicolet 6700 FT-IR.

Results and Discussions

Table 2 summarizes the results for the binding of **1**−**11**. To study the binding we have taken into consideration (1) the anchoring groups, (2) the ZnO material, specifically ZnO−N (nanotips), ZnO−F (films), and ZnO−C (films from colloids), and (3) pH effects. These three factors are addressed in the following sections.

Anchoring Groups. *Carboxylic Acids and Derivatives.* Carboxylic acids and their derivatives (COOMe, COONa, COCl) form stable covalent bonds with metal oxide nanoparticles such as TiO_2, SnO_2, and ZrO_2, mainly through carboxylate bidentate bonds (II and III in Figure 5).[21] Several Ru−polypyridyl dyes have been bound through COOH anchoring groups to ZnO colloidal films prepared by sol−gel methods.[4d−f,21b] On the basis of these results we investigated the binding of **1**, **2**, **4**, **5**, **9**, and **11** including Ru dyes **1** and **2**, to ZnO−N through COOH groups (Table 2).

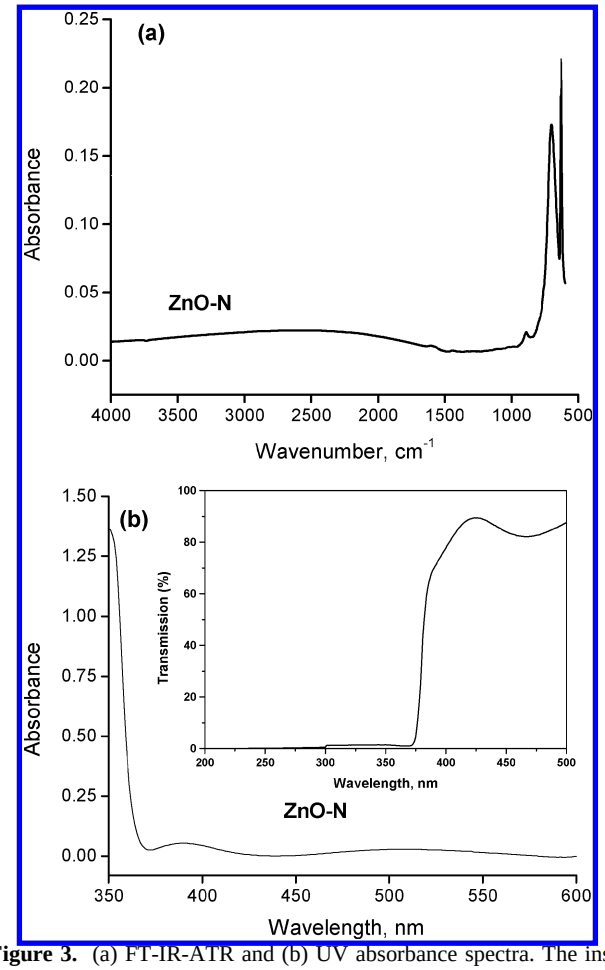

Figure 3. (a) FT-IR-ATR and (b) UV absorbance spectra. The inset shows the transmission of blank ZnO nanotips (ZnO−N) on sapphire.

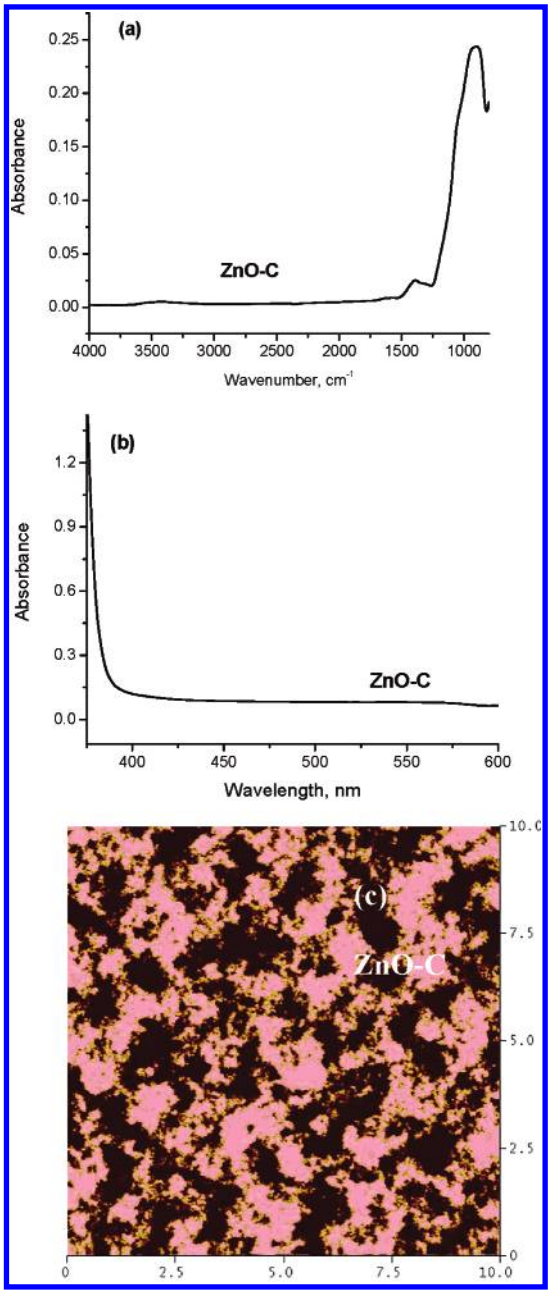

Figure 4. (a) FT-IR-ATR spectrum, (b) UV−vis, and (c) AFM image of a ZnO film prepared from the colloidal solution (ZnO−C).

Ru(II)−polypyridyl complex **2** has been extensively studied together with many of its derivatives for the sensitization of TiO_2 films.[14] The ZnO−N turned from transparent to deep orange after soaking overnight in a 2 mM ethanol or CH_3CN solution of **2**. However, the film became colorless after rinsing with pure solvent, indicating that **2** was weakly physisorbed to the films. Both IR and UV spectra of the rinsed films were identical to those of the films prior to binding. No change in color was observed when ZnO−N was placed overnight in solutions of $Ru(bpy)_3^{2+}$ (**3**), which has no anchoring groups, suggesting that the Ru complex alone does not bind or physisorb.

Ru−polypyridyl rigid-rod **1** is part of a family of rigid-rod dyes that we have developed for TiO_2 sensitization studies.[17a] We have shown that rigid-rod linkers with a *p*-phenylenethynylene $(PhE)_n$ bridge terminating with an isophthalic group and capped with a variety of chromophores, such as Ru complexes,[17a,c] pyrene,[17b] and azulene,[17d] bind effectively to TiO_2 surfaces and can be used as models to study interfacial electron-transfer processes.[17c] Rods made of up to three PhE units (length ∼6−20 Å) and containing a saturated bicyclo[2.2.2.]octyl spacer have been bound to TiO_2 and ZrO_2 films,[17] demonstrating that it is possible to control the length as well as the conjugation of the bridge. The binding of dye **1** to ZnO−N was therefore a proof-of-concept experiment for the functionalization of nanotips with rigid bifunctional linkers.

TABLE 2: Compounds Bound (b), Physisorbed (p), or Nonbound (nb) to ZnO Films

compound	anchoring group	ZnO film[a]	result	detection methods
1[e]	COOH	ZnO−N	b	FT-IR-ATR
		MgZnO−N	b	UV, PL
		ZnO−C	b	
2[d]	COOH	ZnO−N[c]	p	FT-IR-ATR
		ZnO−F[b]	nb	UV, PL
		ZnO−C	b	
3[e]	none	ZnO−N[c]	nb	IR, UV
4	COOH	ZnO−N	b	FT-IR-ATR
5[d]	COOH	ZnO−N	nb[h]	IR
6[f]	$P(O)(OH)_2$	ZnO−N	p[h]	IR
		ZnO−F	nb[h]	
7	$Si(OMe)_3$	ZnO−N	b	FT-IR-ATR
8[g]	$SiCl_3$	ZnO−N	nb[h]	IR
9	COOH	ZnO−N	b	FT-IR-ATR
10[e,g]	SH	ZnO−N	nb	IR
		ZnO−F	nb	
11[e]	COOH	ZnO−N	b	FT-IR-ATR
	and SH	MgZnO−N	b	
		ZnO−F	nb	

[a] ZnO−N = ZnO nanotip films, ZnO−F = ZnO epitaxial films; ZnO−C = ZnO colloidal films, MgZnO−N = $Mg_{0.1}Zn_{0.9}$ nanotip films. [b] Film grown on a sapphire slide. [c] Film grown on a glass slide. [d] Dye solution prepared from EtOH. [e] Dye solution prepared from CH_3CN. [f] Dye solution prepared from H_2O. [g] Dye solution prepared from CH_2Cl_2. [h] Film etched by the acidic solution.

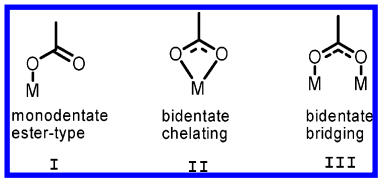

Figure 5. The three main binding modes between a COOH group and a metal oxide surface.

The ZnO−N became orange after soaking 24 h in a 2 mM acetonitrile solution of **1**, and the color persisted after extensive rinsing. UV spectra of these films showed the characteristic broad metal-to-ligand charge-transfer (MLCT) band of the Ru dye centered at ∼470 nm (Figure 6b) while the higher energy π,π^* bands of the bpy ligand overlap with the absorption of the semiconductor.

Static and dynamic quenching of the fluorescence emission of **1** was observed upon binding, as shown in Figures 7a and 7b. This result is expected for dyes that are bound covalently to the semiconductor surface, as the long-lived (microseconds) excited state is rapidly quenched by electron injection into the semiconductor conduction band. These processes are ultrafast, typically a few femtoseconds or a few tenths of femtoseconds for TiO_2,[22a−h] while for ZnO[22f,22i−k] injection rates of ∼100 ps[22f] as well as much shorter rates (<200 fs, for instance)[22i] have been observed.

In our case, the injection rate for **1**/ZnO−N could not be time-resolved with the nanosecond laser (∼10 ns laser pulse). Time-resolved studies at faster time resolutions (∼40 fs) are forthcoming. This will allow a direct comparison of injection rates between **1**/ZnO with the data that we have obtained for **1**/TiO_2.[22l] The availability of both forms of ZnO (colloids and nanotips)

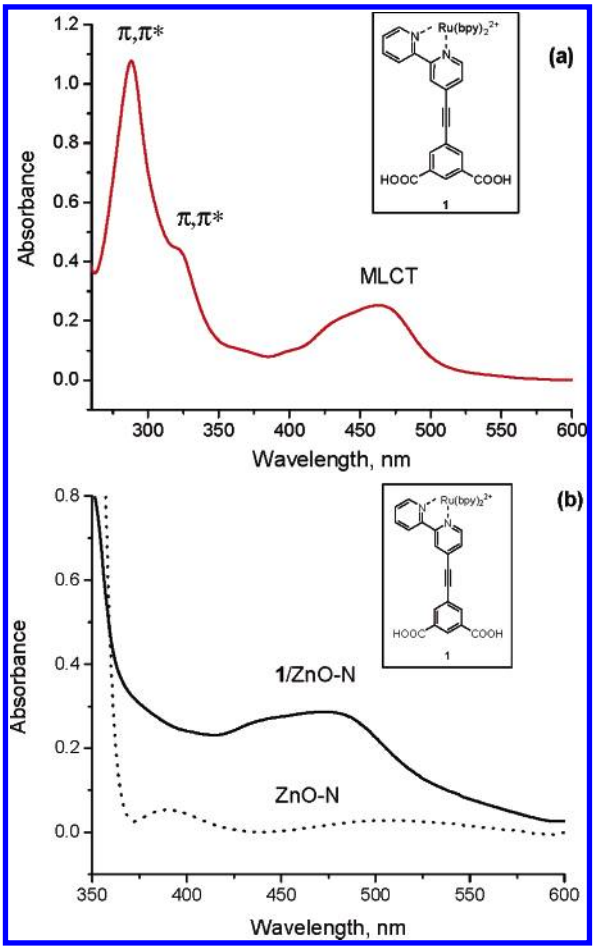

Figure 6. UV spectrum of (a) **1** in CH_3CN solution: $\lambda = 288$ nm, π,π^* of ancillary bpy; $\lambda = 322$ nm, π,π^* of bpy rod linker; $\lambda \approx 470$ nm, MLCT of Ru complex. (b) UV spectrum of **1** bound to ZnO−N on sapphire (solid line) and of the film before binding (dotted line).

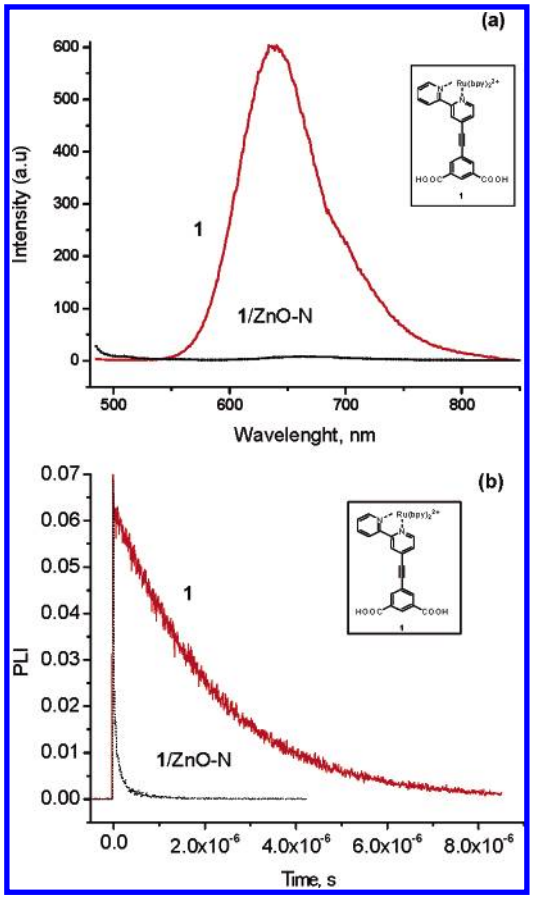

Figure 7. (a) Fluorescence emission spectra of **1** in solution (10^{-6} M in CH_3CN, red solid line), $\lambda_{max} = 636$ nm, and **1** bound to a ZnO−N (black dotted line) ($\lambda_{ex} = 475$ nm). (b) Fluorescence emission decays of **1** in solution (red solid line) and on ZnO nanotips (black dotted line).

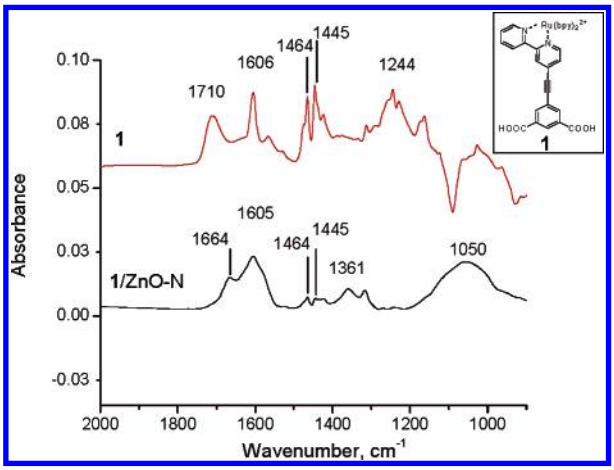

Figure 8. FT-IR-ATR spectra of rigid rod **1** (top, red line) and **1** bound to a ZnO nanotip (bottom, black line).

will also help to determine whether and to what extent different ZnO morphologies and preparations can influence injection rates.

The FT-IR-ATR spectra after binding (Figure 8) clearly indicated the presence of **1** on the film. In general, the FT-IR-ATR spectra of the bound films were considerably weaker than those of the pure compounds, possibly because a relatively small amount of compound binds.

The nature of the chemical bond to the ZnO surface was studied by comparing the FT-IR-ATR spectra of the films of **1** before and after binding to ZnO−N, because binding of the COOH groups as esters or carboxylates to the semiconductor, mainly through the binding modes shown in Figure 5, are known[21] to result in characteristic shifts or spectral changes in the regions of the ν_{as}(C═O) and the ν_{as}(O⋯C⋯O) bands (for the full FT-IR-ATR spectrum of **1**, see Supporting Information, Figure S1).

The FT-IR-ATR spectra in Figure 8 (2000−900 cm^{-1} region) show the disappearance of the ν_{as}(C═O) band at 1710 cm^{-1}, which is present in the spectrum of free **1** (Figure 8, red line) and the appearance of broad bands in the ∼1690−1525 cm^{-1} region upon binding to ZnO−N. These bands are typical of the ν_{as}(O⋯C⋯O) and have been observed in carboxylate bonds to TiO_2 (binding modes II and III in Figure 5).[21] The band at 1606 cm^{-1} in the spectrum of free **1** in Figure 8 was assigned to the C═C stretch of the aromatic rings. This band overlaps with the carboxylate bands in the spectrum of **1**/ZnO−N. The bands at 1464 and 1446 cm^{-1} decreased in intensity upon binding but did not shift. These bands were tentatively assigned to the C═C stretch of the aromatic rings, although COOH and COO^- groups also exhibit bands in that region. Substantial changes were instead observed in the spectral region centered at ∼1245 cm^{-1} (C−O stretch bands). These bands, strong in the spectrum of free **1**, disappeared upon binding. This is interesting because the bands at 1250 cm^{-1}, typically, are not observed in ionized carboxylic salts and carboxylates. In summary, mainly from the changes in the 1714−1600 cm^{-1} carbonyl region, we conclude that both COOH groups of the

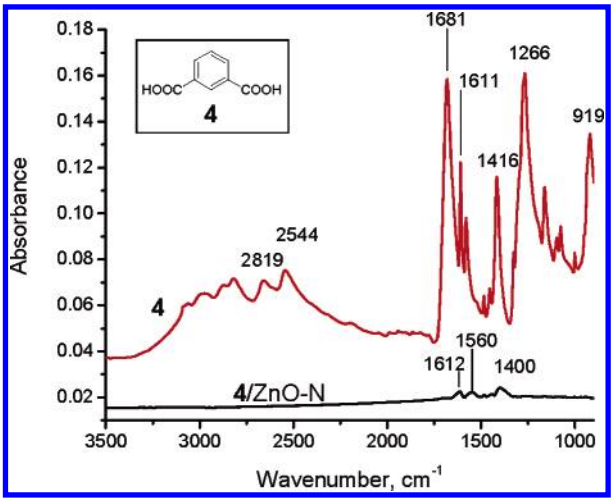

Figure 9. FT-IR-ATR spectrum of isophthalic acid **4** free (top, red line) and bound to ZnO nanotips (bottom, black line).

isophthalic acid unit in **1** bind as a bidentate carboxylate (Figure 5, type II and/or III).

The observation that the Ru−polypyridyl rigid rod binds by the COOH groups while the Ru complex **2** was only weakly physisorbed (Table 2) needs further investigation. The compounds are clearly very similar as they have two COOH binding groups. A possible explanation of this behavior could be a difference in the matching of the anchoring groups with the semiconductor lattice. It is possible that the two COOH groups in the meta position of the benzene ring of **1** are ideally placed so that both bind, while in **2** each COOH in the bpy ring behaves more like an isolated benzoic acid unit. This explanation is consistent with the fact that benzoic acid **5** was a worse binding group than **1**, while isophthalic acid **4** did bind.

Isophthalic acid **4**, used as the reference for the anchoring portion of **1**, was bound to ZnO−N from an 18 mM THF solution, although the film afforded a weak FT-IR-ATR spectrum (Figure 9). Benzoic acid **5** did not bind or physisorb to ZnO−N in a variety of binding conditions (Table 2).

The binding of heptanoic acid **9** was then studied, because aliphatic carboxylic acids with chains of variable length and substituted with a number of different groups ($X-(CH_2)_n-COOH$, $X = NH_2$, SH, etc.) are commercially available. These could be versatile and readily accessible bifunctional linkers for the ZnO nanotips. FT-IR-ATR spectra of the films immersed in a 25 mM solution of **9** in CH_3CN clearly indicated that **9** binds to the films (Figure 10).

After the ZnO−N binding, the C−H stretch bands below 3000 cm^{-1} due to the aliphatic chain did not shift, but the ν(C═O) at 1708 cm^{-1} disappeared with the appearance of a strong new band at 1534 cm^{-1} and a very weak band at 1588 cm^{-1} (the carboxylate asymmetric stretch). In addition, binding resulted in changes in the region of the C−O−H bonds (the 1417 cm^{-1}C−O−H in-plane bending band) and in the disappearance of the ν(C−O) bands at ∼1250 cm^{-1}. The 935 cm^{-1} band, due to the out-of-plane δ(O−H), was absent in the spectrum of **9**/ZnO−N. Finally, the broad O−H stretch at 3300−2500 cm^{-1} in the spectrum of **9** was not observed in the spectrum of **9**/ZnO−N. These changes clearly indicate that COOH group has formed a bond with ZnO−N, probably though carboxylate-type bonds, given the disappearance of the ν(C═O) and the appearance of the asymmetrical stretching bands at ∼1500 cm^{-1}.

Alkylthiols (R−CH₂−SH). Alkanethiols are frequently used to functionalize gold or CdS nanoparticles,[4b,23] and a recent report suggests that thiols do bind to ZnO.[24] Our attempts to

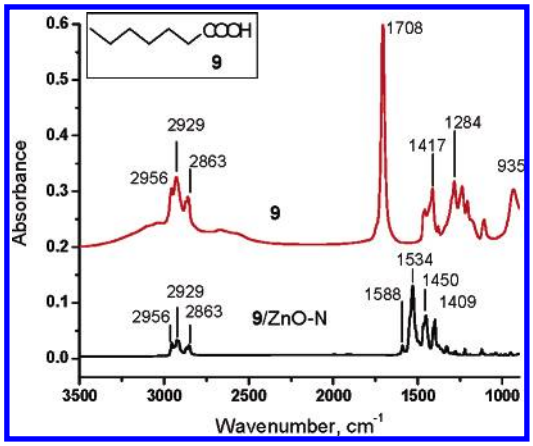

Figure 10. FT-IR-ATR spectra of free heptanoic acid **9** (top, red line) and **9** bound to ZnO nanotips (bottom, black line).

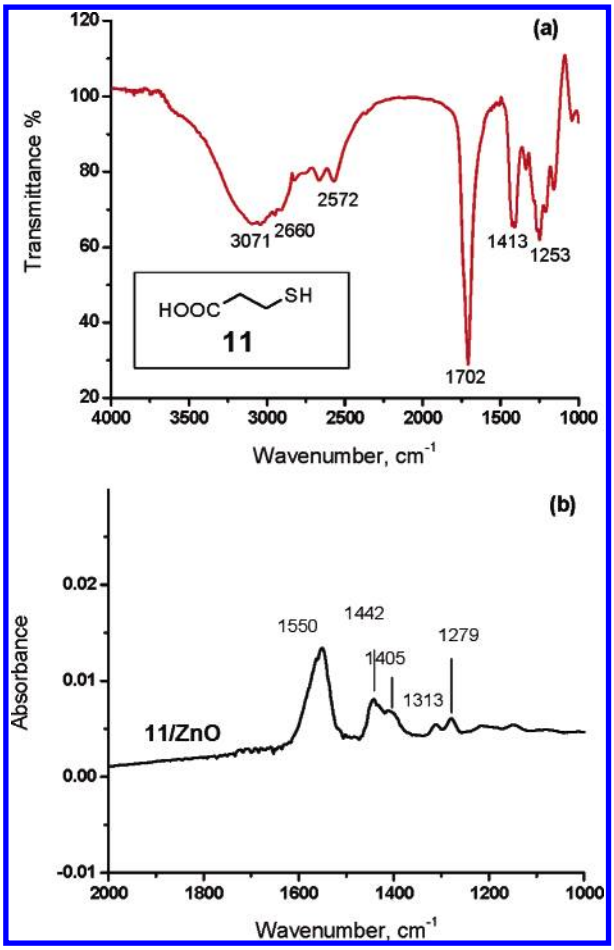

Figure 11. (a) IR spectrum of 3-mercaptopropionic acid (**11**). (b) FT-IR-ATR spectrum of **11** bound to ZnO−N showing the carbonyl region.

bind hexanethiol **10** to the ZnO−N, however, had no success (Table 2) as the FT-IR-ATR spectra of the films before and after binding were identical. 3-Mercaptopropionic acid **11**, however, did bind, as shown by a comparison of the FT-IR spectra before and after binding (Figure 11). The spectrum of **11**/ZnO−N, however, was considerably weak.

Interestingly, the FT-IR-ATR spectrum (2000−1000 cm^{-1} spectral region) of **11**/ZnO−N was remarkably similar to that of hexanoic acid **9**/ZnO−N and so were the spectral changes observed upon binding: In the spectrum of **11**/ZnO−N, the ν-(C═O) band and the strong C−O bands at ∼1250 cm^{-1} disappeared, while new bands due to the carboxylate stretch

were observed in the ~1550 cm^{-1} region.

In conclusion, the binding experiments with **9**−**11** suggest that the binding of 3-mercaptopropionic acid (**11**) to ZnO−N occurs by formation of surface bonds by the COOH group rather than by a bond through the SH group. This indicates that the thiol group in bifunctional **11** is nonbound and could be available for further functionalization of the surface. Although this result appears to be at variance with the only data for thiols on ZnO nanotips available in the literature (the acid binds also through SH),[24] the discrepancy could be due to differences in the ZnO−N film preparation and surface properties. Our own results have shown that these factors can greatly influence binding.

Phosphonic Acid Group R−P(O)(OH)₂. The phosphonic acid group ($R-P(O)(OH)_2$) is an anchoring group widely employed for TiO_2 and other metal oxides.[25] The binding modes to metal oxide surfaces have been studied both experimentally and theoretically, and comparisons with the carboxylate group indicate that phosphonic acids bind more strongly to TiO_2 nanoparticles.[26] The study of $P(O)(OH)_2$ binding was done using phenylphosphonic acid **6**. Our attempts to bind **6** to ZnO−N from 2−20 mM aqueous solutions, however, were not successful, and the films were visibly etched and covered by a white, opaque patina, probably because the phosphonic acid group is too acidic. ZnO nanotips and nanoparticles are readily etched in acidic conditions ($pH \leq 4$),[4d,21b] and phenylphosphonic acid **6** ($pK_{a1} = 2.2$) is a stronger acid than benzoic acid **5** ($pK_a = 4.2$) and isopthalic acid **4** ($pK_{a1} = 3.7$). Also, in the case of benzoic acid **5**, no binding to ZnO−N was observed using 2 mM solutions, but 25 mM solutions etched the films, suggesting that higher concentrations of a weak acid can dissolve the films. In conclusion, the fact that some groups did not bind may be due to an etching process, in which the acidic anchoring group "dissolves" the surface of the nanotips, forming a soluble complex with Zn.[4d]

Silanes Si(X)₃, X = Cl, OR. The trichloro- or trimethoxy silane groups ($Si(X)_3$, X = Cl, OR) anchor to glass, silicon, TiO_2, and indium tin oxide (ITO) and have been used to attach dyes and other molecules to such substrates for a variety of applications.[27] The Si−Cl or Si−OR bonds are labile and form Si−OM bonds upon reaction with MO nanoparticles or surfaces. In addition, many bifunctional alkyl silanes having the structure $R-(CH_2)_n-SiX_3$, where R contains a second functional group, are commercially available. We selected trimethoxy(2-phenylethyl)silane **7** and trichloro(2-phenylethyl)silane **8**, which carried both an alkyl and a phenyl group, thereby allowing us to detect their binding by inspecting the bands characteristic of the aromatic ring and the CH_2 groups in the FT-IR-ATR spectra. Several attempts to bind **8**, however, resulted in complete stripping of the nanotips, as no ZnO was detected (UV, FT-IR) on the sapphire or glass slides after immersing the films in acetonitrile solutions of **8**. Furthermore, etching of the ZnO layer occurred within minutes. We concluded that the solutions of the trichlorosilane were too acidic (pH ~1−0.5). Binding experiments of acetonitrile solutions of the trimethoxysilane **7** to ZnO or ZnMgO nanotips were not successful, but it was possible to bind this molecule after acid pretreatment of the more robust MgZnO films (vide infra).

Effect of ZnO Film Type (ZnO−F, ZnO−N, and ZnO−C) on Binding. In addition to ZnO nanotips (ZnO−N, Figures 2b and 2c), we studied the binding of **1** and **2** to films (ZnO−F, Figure 2a) and to mesoporous films prepared from colloidal ZnO by sol−gel methods (ZnO−C, Figure 4). Significant binding of **1** and **2** to the ZnO−F films could not be detected. This result was not unexpected, given the smaller surface area

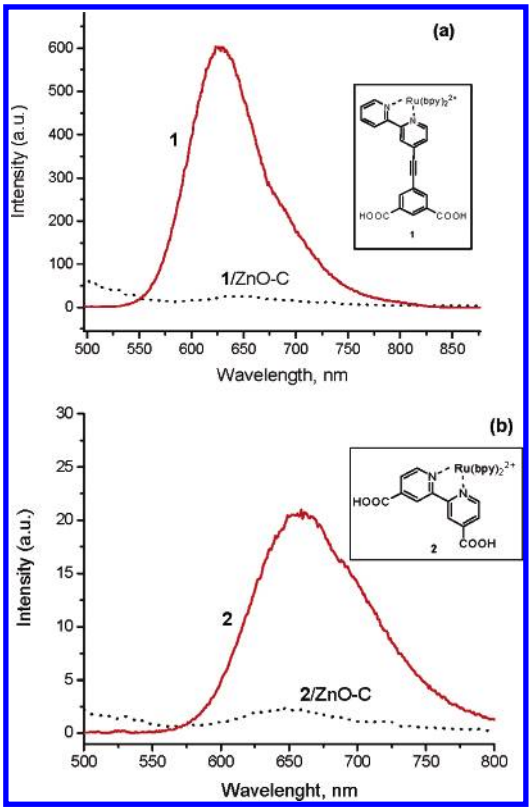

Figure 12. Fluorescence emission spectra of (a) **1** in solution (10^{-6} M in CH_3CN, red solid line), $\lambda_{max} = 636$ nm, and **1** bound to a ZnO−C film (black dotted line) ($\lambda_{ex} = 475$ nm) and (b) **2** in solution (10^{-6} M in CH_3CN, red solid line), $\lambda_{max} = 660$ nm, and **1** bound to a ZnO−C film (black dotted line) ($\lambda_{ex} = 456$ nm).

of flat films compared to the nanotips. Conversely, both complexes **1** and **2** did bind to the ZnO films prepared by colloidal solutions, as shown by the absorption spectra of the films showing the characteristic MLCT band of the complexes (Supporting Information, Figure S2), fluorescence quenching upon binding (Figure 12), and the FT-IR-ATR spectra. (Figure 13)

The nature of the chemical bond between the COOH groups of **1** and **2** and the ZnO surface was studied by comparing their FT-IR-ATR spectra before and after binding (Figure 13). The 2000−900 cm^{-1} spectral region in Figure 13 shows the disappearance of the $\nu_{as}(C{=}O)$ band at 1710 cm^{-1} (Figure 13, spectrum of free **1**) and the appearance of the broad $\nu_{as}(O\cdots C\cdots O)$ bands in the ~1690−1525 cm^{-1} region upon binding. Interestingly, the spectrum of **1** bound to the ZnO−C films is remarkably similar to the spectrum of **1** bound to the ZnO−N nanotips (Figure 8). The ZnO−C films functionalized with **1** were light orange, while the **1**/ZnO−N films were dark orange, suggesting a higher surface coverage in the case of the nanotips. Complex **2**, which physisorbed but did not bind to ZnO−N, was weakly bound to ZnO−C (Figure 13b, black line).

Effect of pH. The treatment of TiO_2 films prepared by sol−gel (hydrothermal) methods with acids or bases prior to binding and the pH of the binding solutions are important factors that influence the binding affinity as well as the type of chemical bonds between a functional group and the surface.[17c,25] For instance, we found that the type of chemical bond that the COOH anchoring group forms with the surface depends on the pH treatment of the TiO_2 film before binding: Pretreatment with acids results in ester-type bonds, and pretreatment with bases forms carboxylate-type bonds.[17] Moreover some molecules that did not bind to acid-pretreated films would bind to films treated

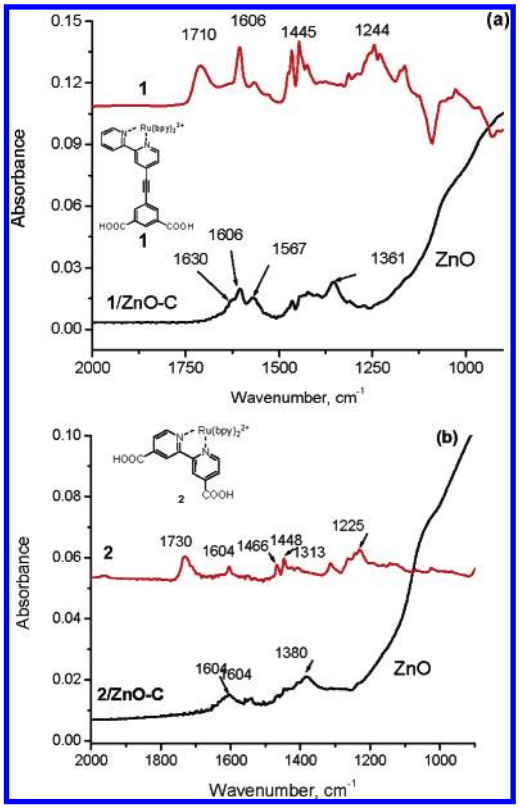

Figure 13. (a) FT-IR-ATR spectra of rigid rod **1** (top, red solid line) and **1** bound to a ZnO−C film (bottom, black solid line) and (b) FT-IR-ATR spectra of rigid rod **2** (top, red solid line) and **2** bound to a ZnO−C film (bottom, black solid line). The films prepared from colloids (ZnO−C) are not transparent in the 1200−800 region.

with base.[17b,c] We then asked ourselves whether this could be observed for ZnO materials.

Since ZnO is readily etched in acidic (pH ≤ 4) conditions, this material could not be employed to test binding at low pH. Lu and co-workers have developed epitaxial $Mg_xZn_{1-x}O$ films by alloying ZnO with MgO[6c,6e] and observed that it is more resistant to acids. $Mg_xZn_{1-x}O$ nanotip films (termed MgZnO−N in this paper) were therefore developed for this work,[28] because they would allow us to employ a wider pH range. The percentage of MgO in alloyed ZnO was varied in the 5−10% range. The preparation of MgZnO−N films will be published elsewhere. We observed that MgZnO−N films have binding properties similar to those of the ZnO−N films. For instance, the IR spectra of **11**/ZnO−N and **11**/MgZnO−N and those of **1**/ZnO−N and **1**/MgZnO−N were indistinguishable (Figures 14 and 15).

The pH pretreatment of MgZnO−N films involved rinsing the slides with deionized water, placing them in an oven at 400 °C for 10 min, followed by cooling and immersion in an acidic or basic aqueous solution for 30 min. Acidic (3 < pH ≤ 5) and basic (8 ≤ pH ≤ 11) aqueous solutions were prepared using H_2SO_4 and NaOH, respectively. These pretreated films were then used in the usual binding procedures (Experimental Procedures section).

Preliminary experiments performed with trimethoxy(2-phenylethyl)silane (**7**), a potentially useful linker that we had been unable to bind to ZnO−N, suggested that an acidic or basic pretreatment of MgZnO−N did influence the binding properties. For instance, **7** did bind to MgZnO−N films that were pretreated with acid (pH 3 and 4) as well as base (pH 9.5), while it did not bind to films (MgZnO−N or ZnO−N) that were not pretreated at all (Supporting Information, Figure S3). A possible

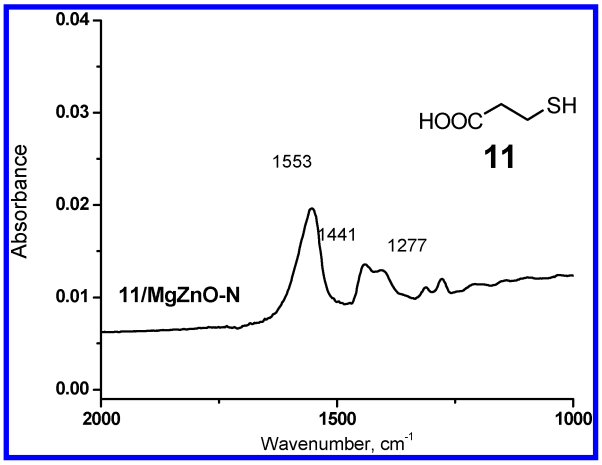

Figure 14. FT-IR-ATR spectrum of **11** bound to MgZnO−N. This spectrum is identical to that of **11**/ZnO−N shown in Figure 11b.

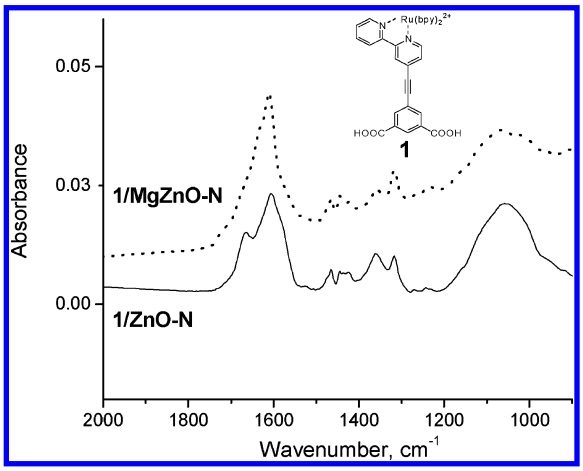

Figure 15. A comparison between FT-IR-ATR spectra of **1** bound to MgZnO−N and ZnO−N films.

explanation for this behavior is that acid or base pretreatment generates defects on the ZnO nanotip surface, making it more reactive. More work will be done to verify this assumption. Clearly, the increased resistance to acids of the MgZnO−N films is potentially very useful, as preliminary experiments suggest that acidic linkers that etched the ZnO nanotips may bind to these more sturdy nanotips.

Conclusions

We have described here the first functionalization of ZnO nanotip films (ZnO−N) with a series mono- or bifunctional linkers and made a comparison between the binding properties of ZnO−N with other ZnO materials (epitaxial films, ZnO−F, and colloidal films, ZnO−C). The binding experiments indicate that the carboxylic acid group (COOH) is a suitable anchoring group for binding to the ZnO−N but that the number and position of the COOH groups, the acidity of the anchoring group, and solution pH also play a role in the binding. The bound films were stable as no changes in the IR, UV, and fluorescence spectra were observed in 1 year old samples. The rigid-rod linkers with two carboxylic anchoring groups and capped with a Ru complex were excellent linkers, and the binding was probed by static and dynamic quenching of the fluorescence as well as by FT-IR-ATR and UV. Since we have demonstrated in our previous work that the Ru complex can be replaced by another dye or small molecule, the rods can be considered useful, and rigid, bifunctional linkers. Another potentially useful, but flexible, bifunctional linker is 3-mercap-

topropionic acid since it did bind by the COOH group, leaving the SH group available for further modifications. The ZnO−N provided excellent binding surfaces when compared to ZnO−F and to the mesoporous ZnO−C films, but the fact that the films are etched at low pH (pH ≤ 4) limits their use. Our experiments suggest that linkers with acidic functional groups "dissolve" the ZnO nanotips. Other explanations to the relatively low reactivity of the ZnO−N are clearly possible, including the fact that the ZnO−N has a highly crystalline, "clean" surface, when compared to the films prepared from colloidal nanoparticles using sol−gel methods. Increased resistance to acids was obtained by alloying ZnO with MgO (5−10%). MgZnO−N films are a novel material that exhibited increased stability toward acidic linkers, while staying identical to the ZnO−N in other respects. Alloyed films could therefore be employed with a larger variety of binding groups and at wider pH ranges. In conclusion, we have demonstrated that ZnO−N can be functionalized with bifunctional linkers. This opens the possibility to develop ZnO−N functionalized with a variety of dyes, redox-active molecules or biomolecules, eventually leading to novel types of anodes for solar cells or to a new ZnO-based integrated, multimode multifunctional sensor technology, which combines different sensing mechanisms (acoustic, electrical, optical, biological, etc.) to achieve higher accuracy and sensitivity and has a broad impact in biological and environmental applications.

Acknowledgment. E. Galoppini is indebted to Professor Dr. Frank Willig for insightful discussions and help in the interpretation of the ZnO binding processes and pH effects. The authors thank Professor Richard Mendelsohn for generously providing access to the FT-IR-ATR and FT-IR instrumentation in his laboratory, Professor Huixin He for AFM data, and Professor Gerald J. Meyer for access to the nanosecond laser. E. Galoppini thanks the Department of Energy, Office of Basic Energy Sciences (Grant No. DE-FG02-01ER15256) for providing the financial support for this work. Yicheng Lu's work has been supported by National Science Foundation under Grant Nos. ECS-0088549, CCR-0103096, and ECS-0224166.

Supporting Information Available: Additional UV and FT-IR spectra of **1**, **2**, and **7**. This material is available free of charge via the Internet at http://pubs.acs.org.

References and Notes

(1) (a) Saito, N.; Haneda, H.; Sekiguchi, T.; Ohashi, N.; Sakaguchi, I.; Koumoto, K. *Adv. Mater.* **2002**, *14*, 418−421. (b) Könenkamp, R.; Word, C. R.; Godinez, M. *Nano Lett.* **2005**, *5*, 2005−2008.

(2) (a) Emanetoglu, N. W.; Zhu, J.; Chen, Y.; Zhong, J.; Chen, Y.; Lu, Y. *Appl. Phys. Lett.* **2004**, *85*, 3702−3704. (b) Liang, S.; Sheng, H.; Liu, Y.; Huo, Z.; Lu, Y.; Shen, H. *J. Cryst. Growth* **2001**, *225*, 110−113.

(3) (a) Mitzner, K. D.; Sternhagen, J.; Galipeau, D. W. *Sens. Actuators, B* **2003**, *93*, 92−99. (b) Kalantar-Zadeh, K.; Wlodarski, W.; Chen, Y. Y.; Fry, B. N.; Galatsis, K. *Sens. Actuators, B* **2003**, *91*, 143−147. (c) Baratto, C.; Sberveglieri, G.; Onischuk, A.; Caruso, B.; di Stasio, S. *Sens. Actuators, B* **2004**, *100*, 261−265. (d) Zhang, F.; Wang, X.; Shiyun, A.; Sun, Z.; Wan, Q.; Zhu, Z.; Xian, Y.; Jin, L.; Yamamoto, K. *Anal. Chim. Acta* **2004**, *519*, 155−160. (e) Zhang, Z.; Emanetoglu, N. W.; Saraf, G.; Chen, Y.; Wu, P.; Zhong, J.; Lu, Y.; Chen, J.; Mirochnitchenko, O.; Inouye, M. *IEEE Trans. Ultrason., Ferroelectr. Freq. Control*, in press.

(4) (a) Liu, W. K.; Salley, M. G.; Gamelin, D. R. *J. Phys. Chem. B* **2005**, *109*, 14486−14495. (b) Lévy-Clément, C.; Tena-Zaera, R.; Ryan, M. A.; Katty, A.; Hodes, G. *Adv. Mater.* **2005**, *17*, 1512−1515. (c) Könenkamp, R.; Boedecker, K.; Lux-Steiner, M. C.; Poschenrieder, M.; Zenia, F.; Lévy-Clément, C.; Wagner, S. *Appl. Phys. Lett.* **2000**, *77*, 2575−2577. (d) Keis, K.; Lindgren, J.; Lindquist, S.-E.; Hagfeldt, A. *Langmuir* **2000**, *16*, 4688−4694. (e) Wang, Z.-S.; Huang, C.-H.; Huang, Y.-Y.; Hou, Y.-J.; Xie, P.-H.; Zhang, B.-W.; Cheng, H.-M. *Chem. Mater.* **2001**, *13*, 678−682. (f) Westermark, K.; Rensmo, H.; Siegbahn, H.; Keis, K.; Hagfeldt, A.; Ojamäe, L.; Persson, P. *J. Phys. Chem. B* **2002**, *106*, 10102−10107.

(5) (a) Gu, Y.; Kuskovsky, I. L.; Yin, M.; O'Brien, S.; Neumark, G. F. *Appl. Phys. Lett.* **2004**, *85*, 3833. (b) Lu, Y.; Zhong, J. In *Semiconductor Nanostructures for Optoelectronic Applications*; Steiner, T., Ed.; Artech House: Boston, 2004; Chapter 6, pp 187−228.

(6) (a) Zhong, J.; Muthukumar, S.; Chen, Y.; Lu, Y.; Ng, H. M.; Jiang, W.; Garfunkel, E. L. *Appl. Phys. Lett.* **2003**, *83*, 3401−3403. (b) Zhang, J.; Zhang, Z.; Wang, T. *Chem. Mater.* **2004**, *16*, 768−770. (c) Muthukumar, S.; Chen, Y.; Zhong, J.; Cosandey, F.; Lu, Y.; Siegrist, T. *J. Cryst. Growth* **2004**, *261*, 316−323. (d) Emanetoglu, N. W.; Muthukumar, S.; Wu, P.; Wittstruck, R.; Chen, Y.; Lu, Y. *IEEE Trans. Ultrason., Ferroelectr. Freq. Control* **2003**, *50*, 537−543. (e) Muthukumar, S.; Zhong, J.; Chen, Y.; Lu, Y.; Siegrist, T. *Appl. Phys. Lett.* **2003**, *82*, 742−744.

(7) (a) Spanhel, L.; Anderson, M. A. *J. Am. Chem. Soc.* **1991**, *113*, 2826−2833. (b) Meulenkamp, E. A. *J. Phys. Chem. B* **1998**, *102*, 5566−5572. (c) Sakohara, S.; Ishida, M.; Anderson, M. A. *J. Phys. Chem. B* **1998**, *102*, 10169−10175. (d) Kamat, P. V.; Patrick, B. *J. Phys. Chem.* **1992**, *96*, 6829−6834. (e) Asadov, A.; Gao, W.; Li, Z.; Lee, J.; Hodgson, M. *Thin Solid Films* **2005**, *476*, 201−205.

(8) (a) Law, M.; Greene, L. E.; Johnson, J. C.; Saykally, R.; Yang, P. *Nat. Mater.* **2005**, *4*, 455−459. (b) Li, Y.; Meng, G. W.; Zhang, L. D.; Phillipp, F. *Appl. Phys. Lett.* **2000**, *76*, 2011−2013. (c) Wang, X.; Song, J.; Li, P.; Ryou, H. J.; Dupuis, D. R.; Summers, C. J.; Wang, Z. L. *J. Am. Chem. Soc.* **2005**, *127*, 7920−7923.

(9) (a) Xu, X. Y.; Zhang, H. Z.; Zhao, Q.; Chen, Y. F.; Xu, J.; Yu, P. D. *J. Phys. Chem. B* **2005**, *109*, 1699−1702. (b) Pan, N.; Wang, X.; Zhang, K.; Hu, H.; Xu, B.; Li, F.; Hou, G. J. *Nanotechnology* **2005**, *16*, 1069−1072. (c) Yi, G.-C.; Wang, C.; Park, W. I. *Semicond. Sci. Technol.* **2005**, *20*, 22−34. (d) Tian, Z. R.; Voigt, J. A.; Mckenzie, B.; Mcdermott, M. *J. Am. Chem. Soc.* **2002**, *124*, 12954−12955.

(10) (a) Lui, R.; Vertegel, A. A.; Bohannan, E. W.; Sorenson, T. A.; Switzer, J. A. *Chem. Mater.* **2001**, *13*, 508−512. (b) Tian, Z. R.; Voigt, J. A.; Mckenzie, B.; Mcdermott, M. J.; Rodriguez, M. A.; Konishi, H.; Xu, H. *Nat. Mater.* **2003**, *2*, 821−826.

(11) (a) Hughess, W. L.; Wang, Z. L. *Appl. Phys. Lett.* **2005**, *86*, 043106. (b) Wen, X.; Fang, Y.; Pang, Q.; Yang, C.; Wang, J.; Ge, W.; Wong, K. S.; Yang, S. *J. Phys. Chem. B* **2005**, *109*, 15303−15308. (c) Pan, Z. W.; Dai, Z. R.; Wang, Z. L. *Science* **2001**, *291*, 1947−1949.

(12) (a) Muthukumar, S.; Sheng, H.; Zhong, J.; Zhang, Z.; Emanetoglu, W. N.; Lu, Y. *IEEE Trans. Nanotechnol.* **2003**, *2*, 50−54. (b) Chen, H.; Zhong, J.; Saraf, G.; Zhang, Z.; Lu, Y.; Fetter, L. A.; Pai, C. *Proc. SPIE−Int. Soc. Opt. Eng.* **2004**, *5592*, 164−169. (c) Zhong, J.; Saraf, G.; Muthukumar, S.; Chen, H.; Chen, Y.; Lu, Y. *J. Electron. Mater.* **2004**, *33*, 654−657.

(13) Fujishima, A.; Honda, K. *Nature.* **1972**, *238*, 37−38.

(14) (a) Kalyanasundaram, K.; Grätzel, M. *Coord. Chem. Rev.* **1998**, *77*, 347−414. (b) Kamat, P. V. *Chem. Rev.* **1993**, *93*, 267−300. (c) Grätzel, M. *Inorg. Chem.* **2005**, *44*, 6841−6851. (d) Meyer, G. J. *Inorg. Chem.* **2005**, *44*, 6852−6864. (e) O'Regan, B.; Grätzel, M. *Nature* **1991**, *353*, 737.

(15) Ogata, K.; Komuro, T.; Hama, K.; Koike, K.; Sasa, S.; Inoue, M.; Yano, M. *Appl. Surf. Sci.* **2004**, *237*, 348−351.

(16) Galoppini, E. *Coord. Chem. Rev.* **2004**, *248*, 1283−1297.

(17) (a) Wang, D.; Schlegel, J. M.; Galoppini, E. *Tetrahedron* **2002**, *58*, 6027−6032. (b) Hoertz, P. G.; Carlisle, R. A.; Meyer G. J.; Wang, D.; Piotrowiak, P.; Galoppini, E. *Nano Lett.* **2003**, *3*, 325−330. (c) Wang, D.; Mendelsohn, R.; Galoppini, E.; Hoertz, P. G.; Carlisle, R. A.; Meyer G. J. *J. Phys. Chem. B* **2004**, *108*, 16642−16653. (d) Lamberto, M.; Pagba, C.; Piotrowiak, P.; Galoppini, E. *Tetrahedron Lett.* **2005**, *46*, 4895.

(18) Gorla, C. R.; Emanetoglu, N. W.; Liang, S.; Mayo, W. E.; Wraback, M.; Shen, H.; Lu, Y. *J. Appl. Phys.* **1999**, *85*, 2595−2602.

(19) Bauer, C.; Boschloo, G.; Mukhtar, E.; Hagfeldt, A. *Chem. Phys. Lett.* **2004**, *387*, 176−181.

(20) Sprintschnik, G.; Sprintschnik, H. W.; Kirsch, P. P.; Whitten, D. G. *J. Am. Chem. Soc.* **1977**, *99*, 4947−4954.

(21) (a) Argazzi, R.; Bignozzi, C. A.; Heimer, T. A.; Castellano, F. N.; Meyer, G. J. *Inorg. Chem.* **1994**, *33*, 5741−5749. (b) Keis, K.; Bauer, C.; Boschloo, G.; Hagfeldt, A.; Westermark, K.; Rensmo, H.; Siegbahn, H. *J. Photochem. Photobiol., A* **2002**, *148*, 57−64. (c) Strommen, D. P.; Mallick, P. K.; Danzer, G. D.; Lumpkin, R. S.; Kincaid, J. R. *J. Phys. Chem.* **1990**, *94*, 1357−1366. (d) Goff, A. H.-L.; Joiret, S.; Falaras, P. *J. Phys. Chem. B* **1999**, *103*, 9569−9575.

(22) (a) Kuciauskas, D.; Monat, J. E.; Villahermosa, R.; Gray, H. B.; Lewis, N. S.; McCusker, J. K. *J. Phys. Chem. B* **2002**, *106*, 9347−9358. (b) Hannappel, T.; Burfeindt, B.; Storck, W.; Willig, F. *J. Phys. Chem. B* **1997**, *101*, 6799−6802. (c) Zimmermann, C.; Willig, F.; Ramakrishna, S.; Burfeindt, B.; Pettinger, B.; Eichberger, R.; Stork, W. *J. Phys. Chem. B* **2001**, *105*, 9245−9253. (d) Benkö, G.; Kallioinen, J.; Korppi-Tommola, E. I.; Yartsev, A.; Sundström, V. *J. Am. Chem. Soc.* **2002**, *124*, 489−493. (e) Benkö, G.; Myllyperkiö, P.; Pan, J.; Yartsev, A. P.; Sundström, V. *J. Am. Chem. Soc.* **2003**, *125*, 1118−1119. (f) Asbury, J. B.; Hao, E.; Wang, Y.; Lian, T. *J. Phys. Chem. B* **2001**, *105*, 4545−4557. (g) Heimer, T. A.;

Heilweil, E. J. *J. Phys. Chem. B* **1997**, *101*, 10990−10993. (h) van't Spijker, H.; Goossens, A. *Thin Solid Films* **2002**, *403*−*404*, 410−414. (i) Bauer, C.; Boschloo, G.; Mukhtar, E.; Hagfeldt, A. *J. Phys. Chem. B* **2001**, *105*, 5585−5588. (j) Asbury, J. B.; Anderson, N. A.; Hao, E.; Ai, X.; Lian, T. *J. Phys. Chem. B* **2003**, *107*, 7376−7386. (k) Persson, P.; Lunell, S.; Ojamäe, L. *Chem. Phys. Lett.* **2002**, *364*, 469−474. (l) Piotrowiak, P.; Myahkostupov, M.; Wang, D.; Galoppini, E., to be submitted for publication.

(23) (a) Daniel, M.-C.; Astruc, D. *Chem. Rev.* **2004**, *104*, 293−346. (b) Tshuruoka, T.; Akamatsu, K.; Nawafune, H. *Langmuir* **2004**, *20*, 11169−11174.

(24) Ogata, K.; Hama, T.; Hama, K.; Koike, K.; Sasa, S.; Inoue, M.; Yano, M. *Appl. Surf. Sci.* **2005**, *241*, 146−149.

(25) Gillaizeau-Gauthier, I.; Odobel, F.; Alebbi, M.; Argazzi, R.; Costa, E.; Bignozzi, A. C.; Qu, P.; Meyer, G. J. *Inorg. Chem.* **2001**, *40*, 6073−6079.

(26) Nilsing, M.; Lunell, S.; Persson, P.; Ojamäe, L. *Surf. Sci.* **2005**, *582*, 49−60.

(27) (a) Helmy, R.; Fadeev, Y. A. *Langmuir* **2002**, *18*, 8924−8928. (b) Li, D.; Ratner, A. M.; Marks, J. T. *J. Am. Chem. Soc.* **1990**, *112*, 7389−7390. (c) Lin, J.; Siddiqui, A. J.; Ottenbrite, M. R. *Polym. Adv. Technol.* **2001**, *12*, 285−292.

(28) Zhong, J.; Saraf, G.; Chen, H.; Lu, Y.; Ng, H. M.; Siegrist, T.; Parekh, A.; Lu, D.; Armour, E. A. In *Proceedings of the 47th Annual TMS Electronic Materials Conference*, Santa Barbara, CA, 2005; p 71.